Sciencexpress Reports

Large-Amplitude Spin Dynamics Driven by a THz Pulse in Resonance with an Electromagnon

T. Kubacka,[1]* J. A. Johnson,[2] M. C. Hoffmann,[3] C. Vicario,[4] S. de Jong,[3] P. Beaud,[2] S. Grübel,[2] S.-W. Huang,[2] L. Huber,[1] L. Patthey,[4] Y.-D. Chuang,[5] J. J. Turner,[3] G. L. Dakovski,[3] W.-S. Lee,[3] M. P. Minitti,[3] W. Schlotter,[3] R. G. Moore,[6] C. P. Hauri,[4,7] S. M. Koohpayeh,[8] V. Scagnoli,[2] G. Ingold,[2] S. L. Johnson,[1] U. Staub[2]

[1]ETH Zurich, Institute for Quantum Electronics, Wolfgang-Pauli-Strasse 16, 8093 Zurich, Switzerland. [2]Swiss Light Source, Paul Scherrer Institut, 5232 Villigen PSI, Switzerland. [3]Linac Coherent Light Source, SLAC National Accelerator Laboratory, Menlo Park, CA94025, USA. [4]SwissFEL, Paul Scherrer Institut, 5232 Villigen PSI, Switzerland. [5]Advanced Light Source, Lawrence Berkeley National Laboratory, Berkeley, CA 94720, USA. [6]Stanford Institute for Materials and Energy Sciences (SIMES), SLAC National Accelerator Laboratory, Menlo Park, CA 94025, USA. [7]Ecole Polytechnique Federale de Lausanne, 1015 Lausanne, Switzerland. [8]Institute for Quantum Matter, Department of Physics and Astronomy, Johns Hopkins University, Baltimore, MD 21218, USA.

*Corresponding author. E-mail: tkubacka@phys.ethz.ch

Multiferroics have attracted strong interest for potential applications where electric fields control magnetic order. The ultimate speed of control via magnetoelectric coupling, however, remains largely unexplored. Here we report on an experiment in which we drive spin dynamics in multiferroic $TbMnO_3$ with an intense few-cycle terahertz (THz) light pulse tuned to resonance with an electromagnon, an electric-dipole active spin excitation. We observe the resulting spin motion using time-resolved resonant soft x-ray diffraction. Our results show that it is possible to directly manipulate atomic-scale magnetic structures using the electric field of light on a sub-picosecond time scale.

Data storage devices based on ferromagnetic or ferroelectric materials depend strongly on domain reorientation, a process that typically occurs over time scales of several nanoseconds. Faster reorientation dynamics may be achievable using intense electromagnetic (EM) pulses (*1*). The EM pulses can couple to magnetism either indirectly via electronic excitations (*2*) or directly via the Zeeman torque induced by the magnetic field (*3–5*). Direct excitation has the advantage of minimal excess heat deposition, but requires frequencies in the 10^{10}-10^{12} Hz range. The low magnetic field strength of currently realizable THz frequency EM sources poses a formidable challenge for such schemes.

Thanks to the coexistence of different ferroic orders, multiferroics offer new routes to domain control (*6*). Particularly strong coupling between the ferroelectric and magnetic order exists in single-phase frustrated magnets where noncollinear spin structure drives ferroelectricity as a result of weak relativistic interactions (*7–9*). Consequently, the magnetic order can be controlled by application of an electric field (*10–13*). The speed of domain switching triggered by simple step-function-like electric fields appears, however, to be limited to a timescale of several milliseconds (*14*). As an alternate solution, optical pulses have been shown to affect the magnetic structure of multiferroics on a femto- and picosecond timescale (*15–17*). It has been predicted that ultrafast magnetic dynamics can be also triggered by coherent excitation of electromagnons, electric-dipole active spin excitations directly connected to the magnetoelectric coupling (*18*). Here we show experimentally that a few-cycle THz pulse tuned to resonance with an electromagnon can transiently modify the magnetic structure of multiferroic $TbMnO_3$.

$TbMnO_3$ is a model spin-cycloid multiferroic exhibiting strong magnetoelectric coupling. Although it has a relatively simple perovskite atomic structure, a strong $GdFeO_3$-type distortion gives rise to a variety of spin-frustrated phases (*19, 20*). At room temperature, the crystal is paramagnetic. Below 42 K the Mn spins form a paraelectric sinusoidally modulated spin density wave (SDW) state which transforms into a spin-cycloid state below 27 K. In this phase the spins form a cycloid within the (*bc*) crystallographic plane (Fig. 1A) and a spontaneous ferroelectric polarization along the *c* axis develops. Microscopically, the spin current between canted spins on neighboring sites *i, j* gives rise to a ferroelectric polarization $\vec{p}_{ij} \propto \vec{r}_{ij} \times \vec{S}_i \times \vec{S}_j$ (*7*), and the magnitude of the polarization is further enhanced by lattice displacements (*21–23*). In all these spin frustrated phases the magnetic structure of the Mn spins is incommensurate with the lattice, characterized by a wave vector $\mathbf{k} = (0,q,0)$, where $q \approx 0.28$ changes very slowly in the SDW phase with temperature (*24*).

The EM excitation spectrum of $TbMnO_3$ shows broad peaks in the THz frequency range; these have been assigned to electromagnons (*25–29*) (Fig. 1B, lower inset). The strongest feature at 1.8 THz is activated with the electric component of light parallel to the *a* axis and is absent in other geometries (*26*). It has been proposed that the oscillating electric field along the *a* axis modifies the nearest neighbor ferromagnetic exchange constant in the (*ab*) plane, resulting in anti-phase spin oscillations within the spin cycloid plane (*28, 30*). Weaker spectral features at lower frequencies have been proposed to arise from the higher harmonics of the spin cycloid and coupling to the strongest electromagnon (*30*), and from out-of-plane spin cycloid motions (*28, 31, 32*).

To investigate whether excitation of electromagnons in $TbMnO_3$ is a viable route for magnetic order control, we performed a THz pump and soft x-ray probe experiment (Fig. 1B). The sample is a single crystal of $TbMnO_3$ cut to the (010) surface, oriented so that the *a* axis is at 45° with respect to the horizontal scattering plane. We generated few-cycle, phase stable THz pulses with a center frequency of 1.8 THz using optical rectification in a nonlinear organic crystal with a peak electric field of approximately 300 kV/cm at focus (*33*). We measured the electric field component of the THz waveform at the sample position using electro-optical sampling. To see the spin motion resulting from the excitation we used time-resolved resonant soft x-ray diffraction at the Mn L_2 edge and measured the intensity of the first order (0*q*0) cycloid reflection (*34*).

The spin dynamics can be extracted from the behavior of the intensity of the (0*q*0) diffraction peak as a function of pump-probe delay time $\Delta\tau$ (Fig. 2). At T = 13 K, where $TbMnO_3$ is deep in the multiferroic phase, the x-ray signal shows oscillations resembling the shape of the THz pump pulse electric field (Fig. 2A). The observed modulation of the diffraction peak intensity is over an order of magnitude larger than expected for unconstrained spin precession driven directly by the magnetic field component of the THz pulse (*34*). The Fourier transform of the x-ray trace (Fig. 2D) shows that the material response has essentially the

same frequency spectrum as both the pump and the electromagnon. The delay between the first maximum of the pump trace and the first maximum of the x-ray trace is 250 fs, corresponding to approximately half of a single oscillation cycle. Inverting the sign of the electric field of the pump pulse results in an opposite sign of changes in the diffraction intensity transients (Fig. 2B). Such behavior is expected when it is the electric field, and not simple heating, that drives the spin motion. When $TbMnO_3$ is in the non-multiferroic SDW phase (T = 30 K), the oscillation in the peak intensity following the pump is strongly suppressed (Fig. 2C). This temperature dependence gives strong evidence that the THz-induced spin motion is correlated with the presence of multiferroicity. At 30 K we tentatively attribute the slight drop of overall intensity after the pump to heating effects from absorption of the THz pulse, which leads to an estimated temperature increase of less than 0.05 K (*34*).

To better understand the time dependence of the spin response, we construct a very simple model of the system as two independent simple harmonic oscillators at the electromagnon resonance frequencies of 0.7 THz and 1.8 THz (*34*). Although not a perfect match to the data, the behavior of the conjugate momentum of the higher frequency oscillator successfully reproduces the general shape of the oscillation and the delay between the driving electric field and the changes in x-ray diffraction (Fig. 2A and 2B). The agreement is much worse for either canonical coordinate of the lower frequency oscillator, suggesting that off-resonant excitation of the lower energy electromagnon or other purely magnetic modes is not consistent with the measured shape or delay of the response (*34*).

Resonant x-ray scattering at the Mn *L*-edge is predominantly sensitive to the magnetic moment of the Mn 3*d* shell (*35*). An analysis of how different spin motions contribute to the intensity of the diffraction peak allows us to test which of them are involved in the observed oscillations. We consider two components of the induced spin motion, motivated by the current understanding of spin dynamics in this system. In the first component the spins move in antiphase within the spin cycloid plane, the pattern widely considered to be responsible for the infrared activity of the 1.8 THz electromagnon (*28*). The driving electric field applies an effective "force" to this component. In our model of the electromagnon as a harmonic oscillator, this component of the spin motion should then be identified with the "position" of the oscillator. In the proposed pure spin Hamiltonian for this system (*18*), the conjugate momentum must be a spin motion orthogonal to this position coordinate. Numerical simulations based on this Hamiltonian have predicted that a sufficiently intense THz pulse in resonance with the 1.8 THz electromagnon can induce coherent rotation of the spin cycloid plane about the *b* axis until it reaches another stable orientation in either the (*ab*) or (*bc*) plane (*18*). In our experiment the effective THz pulse field strength is over two orders of magnitude lower than used in these simulations (*34*) and so we do not expect to see a persistent domain reorientation. Instead, we propose to consider a smaller rotation of the spin cycloid plane about the *b* axis as a second component of the spin motion that corresponds to the conjugate momentum for the 1.8 THz resonance.

We model these two spin motion patterns separately as distortions to the equilibrium magnetic structure which influence the magnetic structure factor (*34*). We then calculate the intensity of the (0q0) diffraction peak as a function of each coordinate of the spin motion (Fig. 3). For the in-plane motion the intensity of the diffraction peak is an even function of the spin coordinate, giving a decrease of the diffracted intensity with twice the frequency of the spin motion (Fig. 3A). For the spin cycloid plane rotation, the change of diffracted intensity is an odd function of the rotation angle. This motion then leads to a modulation of the diffraction intensity with the same frequency as the spin motion (Fig. 3B). For a field-driven excitation process we expect the spin motion frequency to be the same as the frequency of THz pump. We conclude that the main motion visible in our experiment is a rotation of the spin cycloid plane. The in-plane spin motion may also be present, but its response would be suppressed at the current experimental time resolution. This is consistent with our harmonic oscillator model, which suggests that we see primarily dynamics of the conjugate momentum of the resonance.

For π-polarized x-rays at the Mn L_2 edge the scattering intensity is a strongly varying function of the sample azimuth (rotation about the Bragg wave vector) (*34*). Rotation of the spin cycloid plane about the *b* axis induced by the THz pulse is equivalent to rotating the sample about the (0q0) scattering vector. Hence we interpret the data quantitatively by comparing the change of the intensity of the diffraction peak seen in the pump-probe trace with the change seen upon rotating the sample by a small angle around the azimuth of 45° in equilibrium conditions (Fig. 4). We estimate that the observed (1.35 ± 0.12)% maximum change of peak intensity corresponds to an amplitude of spin cycloid plane rotation equal to (4.2 ± 0.4)° (*34*). We expect higher fields will lead to larger spin cycloid rotations. A simple linear extrapolation suggests that THz pulses with an amplitude of 1-2 MV/cm inside the sample could lead to spin cycloid rotations on the order of 90°. We can compare this against the model of Ref. (*18*), which predicts switching at 14-15 MV/cm for single-cycle THz pulses.

Our results show that intense THz pulses can modify the magnetic order in a multiferroic. Given that $TbMnO_3$ is a model compound for a large group of materials with noncollinear spin order, our results serve as a proof-of-principle for a wide range of compounds. Moreover, the presence of magnetoelectric coupling in multiferroic heterostructures encourages a search for similar mechanisms as a basis for technologically feasible multiferroic devices.

References and Notes

1. E. Beaurepaire, J. Merle, A. Daunois, J. Bigot, Ultrafast spin dynamics in ferromagnetic nickel. *Phys. Rev. Lett.* **76**, 4250–4253 (1996). Medline doi:10.1103/PhysRevLett.76.4250
2. A. Kirilyuk, A. V. Kimel, T. Rasing, Ultrafast optical manipulation of magnetic order. *Rev. Mod. Phys.* **82**, 2731–2784 (2010). doi:10.1103/RevModPhys.82.2731
3. T. Kampfrath, A. Sell, G. Klatt, A. Pashkin, S. Mährlein, T. Dekorsy, M. Wolf, M. Fiebig, A. Leitenstorfer, R. Huber, Coherent terahertz control of antiferromagnetic spin waves. *Nat. Photonics* **5**, 31–34 (2011). doi:10.1038/nphoton.2010.259
4. K. Yamaguchi, M. Nakajima, T. Suemoto, Coherent control of spin precession motion with impulsive magnetic fields of half-cycle terahertz radiation. *Phys. Rev. Lett.* **105**, 237201 (2010). Medline doi:10.1103/PhysRevLett.105.237201
5. C. Vicario, C. Ruchert, F. Ardana-Lamas, P. M. Derlet, B. Tudu, J. Luning, C. P. Hauri, Off-resonant magnetization dynamics phase-locked to an intense phase-stable terahertz transient. *Nat. Photonics* **7**, 720–723 (2013). doi:10.1038/nphoton.2013.209
6. W. Eerenstein, N. D. Mathur, J. F. Scott, Multiferroic and magnetoelectric materials. *Nature* **442**, 759–765 (2006). Medline doi:10.1038/nature05023
7. H. Katsura, N. Nagaosa, A. V. Balatsky, Spin current and magnetoelectric effect in noncollinear magnets. *Phys. Rev. Lett.* **95**, 057205 (2005). Medline doi:10.1103/PhysRevLett.95.057205
8. M. Mostovoy, Ferroelectricity in spiral magnets. *Phys. Rev. Lett.* **96**, 067601 (2006). Medline doi:10.1103/PhysRevLett.96.067601
9. S.-W. Cheong, M. Mostovoy, Multiferroics: A magnetic twist for ferroelectricity. *Nat. Mater.* **6**, 13–20 (2007). Medline doi:10.1038/nmat1804
10. T. Lottermoser, T. Lonkai, U. Amann, D. Hohlwein, J. Ihringer, M. Fiebig, Magnetic phase control by an electric field. *Nature* **430**, 541–544 (2004). Medline doi:10.1038/nature02728
11. Y. Bodenthin, U. Staub, M. García-Fernández, M. Janoschek, J. Schlappa, E. I. Golovenchits, V. A. Sanina, S. G. Lushnikov, Manipulating the magnetic structure with electric fields in multiferroic $ErMn_2O_5$. *Phys. Rev. Lett.* **100**, 027201 (2008). Medline doi:10.1103/PhysRevLett.100.027201
12. Y. Yamasaki, H. Sagayama, T. Goto, M. Matsuura, K. Hirota, T. Arima, Y. Tokura, Electric control of spin helicity in a magnetic ferroelectric. *Phys. Rev. Lett.* **98**, 147204 (2007). Medline doi:10.1103/PhysRevLett.98.147204
13. Y. J. Choi, C. L. Zhang, N. Lee, S. W. Cheong, Cross-control of

magnetization and polarization by electric and magnetic fields with competing multiferroic and weak-ferromagnetic phases. *Phys. Rev. Lett.* **105**, 097201 (2010). Medline doi:10.1103/PhysRevLett.105.097201
14. T. Hoffmann, P. Thielen, P. Becker, L. Bohatý, M. Fiebig, Time-resolved imaging of magnetoelectric switching in multiferroic $MnWO_4$. *Phys. Rev. B* **84**, 184404 (2011). doi:10.1103/PhysRevB.84.184404
15. S. L. Johnson, R. A. de Souza, U. Staub, P. Beaud, E. Möhr-Vorobeva, G. Ingold, A. Caviezel, V. Scagnoli, W. F. Schlotter, J. J. Turner, O. Krupin, W. S. Lee, Y. D. Chuang, L. Patthey, R. G. Moore, D. Lu, M. Yi, P. S. Kirchmann, M. Trigo, P. Denes, D. Doering, Z. Hussain, Z. X. Shen, D. Prabhakaran, A. T. Boothroyd, Femtosecond dynamics of the collinear-to-spiral antiferromagnetic phase transition in CuO. *Phys. Rev. Lett.* **108**, 037203 (2012). Medline doi:10.1103/PhysRevLett.108.037203
16. I. P. Handayani, R. I. Tobey, J. Janusonis, D. A. Mazurenko, N. Mufti, A. A. Nugroho, M. O. Tjia, T. T. Palstra, P. H. van Loosdrecht, Dynamics of photo-excited electrons in magnetically ordered $TbMnO_3$. *J. Phys. Condens. Matter* **25**, 116007 (2013). Medline doi:10.1088/0953-8984/25/11/116007
17. D. S. Rana, I. Kawayama, K. Mavani, K. Takahashi, H. Murakami, M. Tonouchi, Understanding the nature of ultrafast polarization dynamics of ferroelectric memory in the multiferroic $BiFeO_3$. *Adv. Mater.* **21**, 2881–2885 (2009). doi:10.1002/adma.200802094
18. M. Mochizuki, N. Nagaosa, Theoretically predicted picosecond optical switching of spin chirality in multiferroics. *Phys. Rev. Lett.* **105**, 147202 (2010). Medline doi:10.1103/PhysRevLett.105.147202
19. T. Kimura, T. Goto, H. Shintani, K. Ishizaka, T. Arima, Y. Tokura, Magnetic control of ferroelectric polarization. *Nature* **426**, 55–58 (2003). Medline doi:10.1038/nature02018
20. M. Kenzelmann, A. B. Harris, S. Jonas, C. Broholm, J. Schefer, S. B. Kim, C. L. Zhang, S. W. Cheong, O. P. Vajk, J. W. Lynn, Magnetic inversion symmetry breaking and ferroelectricity in $TbMnO_3$. *Phys. Rev. Lett.* **95**, 087206 (2005). Medline doi:10.1103/PhysRevLett.95.087206
21. I. A. Sergienko, E. Dagotto, Role of the Dzyaloshinskii-Moriya interaction in multiferroic perovskites. *Phys. Rev. B* **73**, 094434 (2006). doi:10.1103/PhysRevB.73.094434
22. A. Malashevich, D. Vanderbilt, First principles study of improper ferroelectricity in $TbMnO_3$. *Phys. Rev. Lett.* **101**, 037210 (2008). Medline doi:10.1103/PhysRevLett.101.037210
23. H. C. Walker, F. Fabrizi, L. Paolasini, F. de Bergevin, J. Herrero-Martin, A. T. Boothroyd, D. Prabhakaran, D. F. McMorrow, Femtoscale magnetically induced lattice distortions in multiferroic $TbMnO_3$. *Science* **333**, 1273–1276 (2011). Medline doi:10.1126/science.1208085
24. S. B. Wilkins, T. R. Forrest, T. A. Beale, S. R. Bland, H. C. Walker, D. Mannix, F. Yakhou, D. Prabhakaran, A. T. Boothroyd, J. P. Hill, P. D. Hatton, D. F. McMorrow, Nature of the magnetic order and origin of induced ferroelectricity in $TbMnO_3$. *Phys. Rev. Lett.* **103**, 207602 (2009). Medline doi:10.1103/PhysRevLett.103.207602
25. A. Pimenov, A. A. Mukhin, V. Y. Ivanov, V. D. Travkin, A. M. Balbashov, A. Loidl, Possible evidence for electromagnons in multiferroic manganites. *Nat. Phys.* **2**, 97–100 (2006). doi:10.1038/nphys212
26. Y. Takahashi, N. Kida, Y. Yamasaki, J. Fujioka, T. Arima, R. Shimano, S. Miyahara, M. Mochizuki, N. Furukawa, Y. Tokura, Evidence for an electric-dipole active continuum band of spin excitations in multiferroic $TbMnO_3$. *Phys. Rev. Lett.* **101**, 187201 (2008). Medline doi:10.1103/PhysRevLett.101.187201
27. A. Pimenov, A. Shuvaev, A. Loidl, F. Schrettle, A. A. Mukhin, V. D. Travkin, V. Y. Ivanov, A. M. Balbashov, Magnetic and magnetoelectric excitations in $TbMnO_3$. *Phys. Rev. Lett.* **102**, 107203 (2009). Medline doi:10.1103/PhysRevLett.102.107203
28. R. Valdés Aguilar, M. Mostovoy, A. B. Sushkov, C. L. Zhang, Y. J. Choi, S. W. Cheong, H. D. Drew, Origin of electromagnon excitations in multiferroic $RMnO_3$. *Phys. Rev. Lett.* **102**, 047203 (2009). Medline doi:10.1103/PhysRevLett.102.047203
29. P. Rovillain, M. Cazayous, Y. Gallais, M. A. Measson, A. Sacuto, H. Sakata, M. Mochizuki, Magnetic field induced dehybridization of the electromagnons in multiferroic $TbMnO_3$. *Phys. Rev. Lett.* **107**, 027202 (2011). Medline doi:10.1103/PhysRevLett.107.027202
30. M. Mochizuki, N. Furukawa, N. Nagaosa, Theory of electromagnons in the multiferroic Mn perovskites: The vital role of higher harmonic components of the spiral spin order. *Phys. Rev. Lett.* **104**, 177206 (2010). Medline doi:10.1103/PhysRevLett.104.177206
31. H. Katsura, A. V. Balatsky, N. Nagaosa, Dynamical magnetoelectric coupling in helical magnets. *Phys. Rev. Lett.* **98**, 027203 (2007). Medline doi:10.1103/PhysRevLett.98.027203
32. A. M. Shuvaev, V. D. Travkin, V. Y. Ivanov, A. A. Mukhin, A. Pimenov, Evidence for electroactive excitation of the spin cycloid in $TbMnO_3$. *Phys. Rev. Lett.* **104**, 097202 (2010). Medline doi:10.1103/PhysRevLett.104.097202
33. C. Ruchert, C. Vicario, C. P. Hauri, Spatiotemporal focusing dynamics of intense supercontinuum THz pulses. *Phys. Rev. Lett.* **110**, 123902 (2013). doi:10.1103/PhysRevLett.110.123902
34. See supplementary materials.
35. S. W. Lovesey, S. P. Collins, *X-ray Scattering and Absorption by Magnetic Materials* (Clarendon, Oxford, 1996).
36. W. F. Schlotter, J. J. Turner, M. Rowen, P. Heimann, M. Holmes, O. Krupin, M. Messerschmidt, S. Moeller, J. Krzywinski, R. Soufli, M. Fernández-Perea, N. Kelez, S. Lee, R. Coffee, G. Hays, M. Beye, N. Gerken, F. Sorgenfrei, S. Hau-Riege, L. Juha, J. Chalupsky, V. Hajkova, A. P. Mancuso, A. Singer, O. Yefanov, I. A. Vartanyants, G. Cadenazzi, B. Abbey, K. A. Nugent, H. Sinn, J. Lüning, S. Schaffert, S. Eisebitt, W. S. Lee, A. Scherz, A. R. Nilsson, W. Wurth, The soft x-ray instrument for materials studies at the linac coherent light source x-ray free-electron laser. *Rev. Sci. Instrum.* **83**, 043107 (2012). Medline doi:10.1063/1.3698294
37. D. Doering, Y. D. Chuang, N. Andresen, K. Chow, D. Contarato, C. Cummings, E. Domning, J. Joseph, J. S. Pepper, B. Smith, G. Zizka, C. Ford, W. S. Lee, M. Weaver, L. Patthey, J. Weizeorick, Z. Hussain, P. Denes, Development of a compact fast CCD camera and resonant soft x-ray scattering endstation for time-resolved pump-probe experiments. *Rev. Sci. Instrum.* **82**, 073303 (2011). Medline doi:10.1063/1.3609862
38. S. W. Lovesey, V. Scagnoli, M. Garganourakis, S. M. Koohpayeh, C. Detlefs, U. Staub, Melting of chiral order in terbium manganate ($TbMnO_3$) observed with resonant x-ray Bragg diffraction. *J. Phys. Condens. Matter* **25**, 362202 (2013). Medline doi:10.1088/0953-8984/25/36/362202
39. Z. Yang, L. Mutter, M. Stillhart, B. Ruiz, S. Aravazhi, M. Jazbinsek, A. Schneider, V. Gramlich, P. Günter, Large-size bulk and thin-film stilbazolium-salt single crystals for nonlinear optics and THz generation. *Adv. Funct. Mater.* **17**, 2018–2023 (2007). doi:10.1002/adfm.200601117
40. P. C. M. Planken, H.-K. Nienhuys, H. J. Bakker, T. Wenckebach, Measurement and calculation of the orientation dependence of terahertz pulse detection in ZnTe. *J. Opt. Soc. Am. B* **18**, 313 (2001). doi:10.1364/JOSAB.18.000313
41. M. C. Hoffmann, J. A. Fülöp, Intense ultrashort terahertz pulses: Generation and applications. *J. Phys. D Appl. Phys.* **44**, 083001 (2011). doi:10.1088/0022-3727/44/8/083001
42. H. Hirori, A. Doi, F. Blanchard, K. Tanaka, Single-cycle terahertz pulses with amplitudes exceeding 1 MV/cm generated by optical rectification in $LiNbO_3$. *Appl. Phys. Lett.* **98**, 091106 (2011). doi:10.1063/1.3560062
43. N. Kida, Y. Takahashi, J. S. Lee, R. Shimano, Y. Yamasaki, Y. Kaneko, S. Miyahara, N. Furukawa, T. Arima, Y. Tokura, Terahertz time-domain spectroscopy of electromagnons in multiferroic perovskite manganites. *J. Opt. Soc. Am. B* **26**, A35 (2009). doi:10.1364/JOSAB.26.000A35
44. M. Beye, O. Krupin, G. Hays, A. H. Reid, D. Rupp, S. Jong, S. Lee, W.-S. Lee, Y.-D. Chuang, R. Coffee, J. P. Cryan, J. M. Glownia, A. Föhlisch, M. R. Holmes, A. R. Fry, W. E. White, C. Bostedt, A. O. Scherz, H. A. Durr, W. F. Schlotter, X-ray pulse preserving single-shot optical cross-correlation method for improved experimental temporal resolution. *Appl. Phys. Lett.* **100**, 121108 (2012). doi:10.1063/1.3695164
45. J. M. Fornies-Marquina, J. Letosa, M. Garcia-Gracia, J. M. Artacho, Error propagation for the transformation of time domain into frequency domain. *IEEE Trans. Magn.* **33**, 1456–1459 (1997). doi:10.1109/20.582534
46. U. Staub, V. Scagnoli, Y. Bodenthin, M. García-Fernández, R. Wetter, A. M. Mulders, H. Grimmer, M. Horisberger, Polarization analysis in soft X-ray diffraction to study magnetic and orbital ordering. *J. Synchrotron Radiat.* **15**, 469–476 (2008). Medline doi:10.1107/S0909049508019614
47. J. P. Hill, D. F. McMorrow, Resonant exchange scattering: Polarization dependence and correlation function. *Acta Crystallogr. A* **52**, 236–244 (1996). doi:10.1107/S0108767395012670

Acknowledgments: This research was carried out on the SXR Instrument at the LCLS, a division of SLAC and an Office of Science user facility operated by Stanford University for the U.S. Department of Energy (DOE). The SXR

Instrument is funded by a consortium including the LCLS, Stanford University through SIMES, LBNL, the University of Hamburg through the BMBF priority program FSP 301, and the Center for Free Electron Laser Science (CFEL). This research was supported by the NCCR MUST and NCCR MaNEP, funded by the Swiss National Science Foundation, and by the Swiss National Science Foundation (Grant No. 200021_144115). Our ultrafast activities are supported by the ETH Femtosecond and Attosecond Science and Technology (ETH-FAST) initiative as part of the NCCR MUST program. The Advanced Light Source is supported by DOE under contract No. DE-AC02-05CH11231. Crystal growth work at IQM was supported by DOE, Office of Basic Energy Sciences, Division of Materials Sciences and Engineering under Award DE-FG02-08ER46544. W.-S. L., Y.-D. C., and R. G. M. are supported by the Department of Energy, Office of Basic Energy Sciences, Materials Sciences and Engineering Division, under contract DE-AC02-76SF00515. S. L. J. and U. S. contributed equally to this work.

Supplementary Materials
www.sciencemag.org/cgi/content/full/science.1242862/DC1
Materials and Methods
Supplementary Text
Figs. S1 to S3
References (*36*–*47*)

8 July 2013; accepted 19 February 2014
Published online 6 March 2014
10.1126/science.1242862

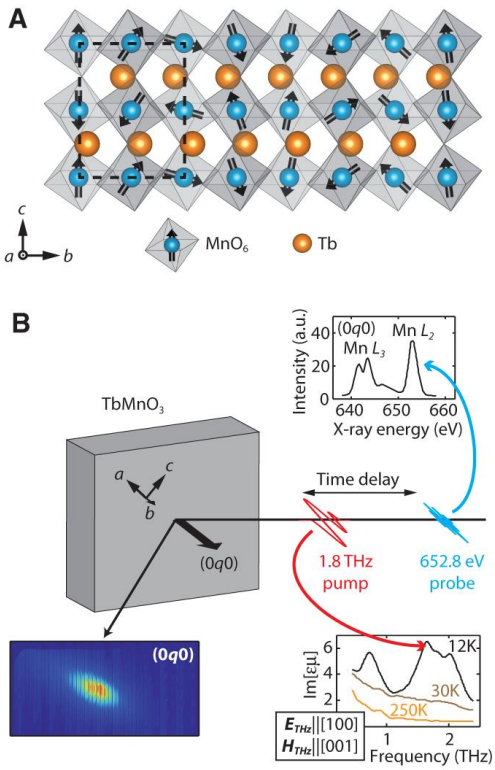

Fig. 1. Experimental setup. (**A**) The magnetic structure of $TbMnO_3$ below 27 K. The spins of the Mn 3*d* shells (black arrows) form a cycloid propagating within the (*bc*) crystallographic plane. The oxygens are represented by gray octahedra around the Mn atoms (blue spheres). The black dashed box indicates a unit cell. (**B**) Schematic of the experiment. A THz pulse resonant with the strongest electromagnon [lower right inset (*26*)] excites spin motion in the sample. An x-ray pulse resonant with the Mn L_2 edge (upper inset) measures the response as changes in the intensity of the (0*q*0) diffraction peak (lower left inset).

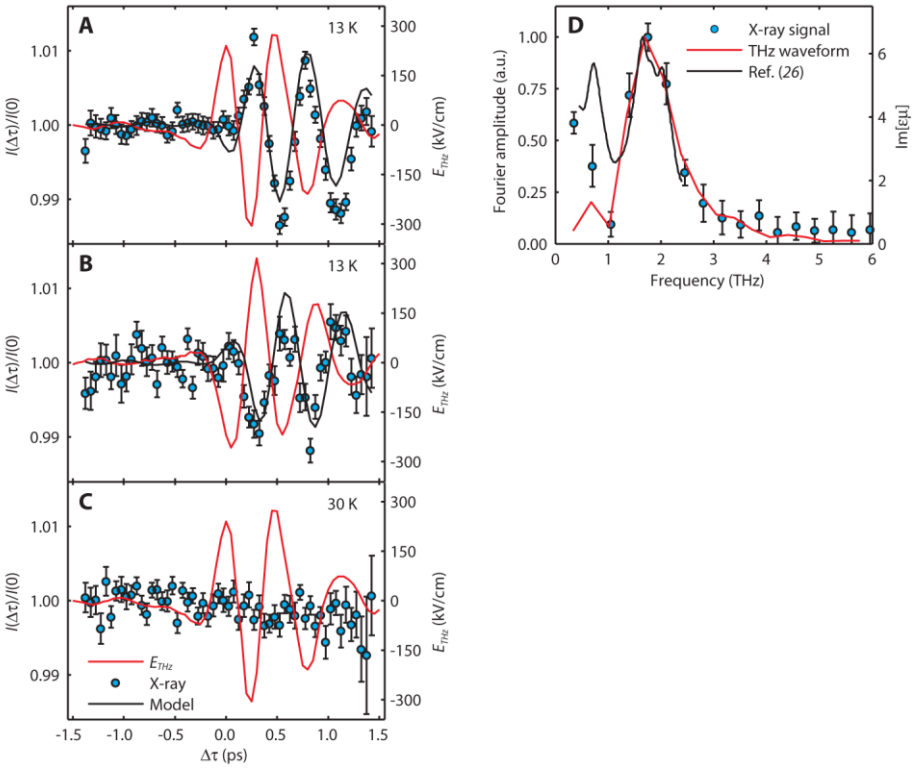

Fig. 2. Time-dependent behavior. The magnetic diffraction intensity of the (0*q*0) peak of $TbMnO_3$ (blue symbols, left axis), compared with the pump trace (red solid line, right axis) as a function of the time delay. (**A** and **B**) The response of the crystal in the multiferroic phase (T = 13 K) for opposite signs of the driving electric field. The solid black lines are based on a model discussed in the text. (**C**) The response in the SDW phase (T = 30 K). (**D**) Fourier transform of the THz and x-ray traces from (A).

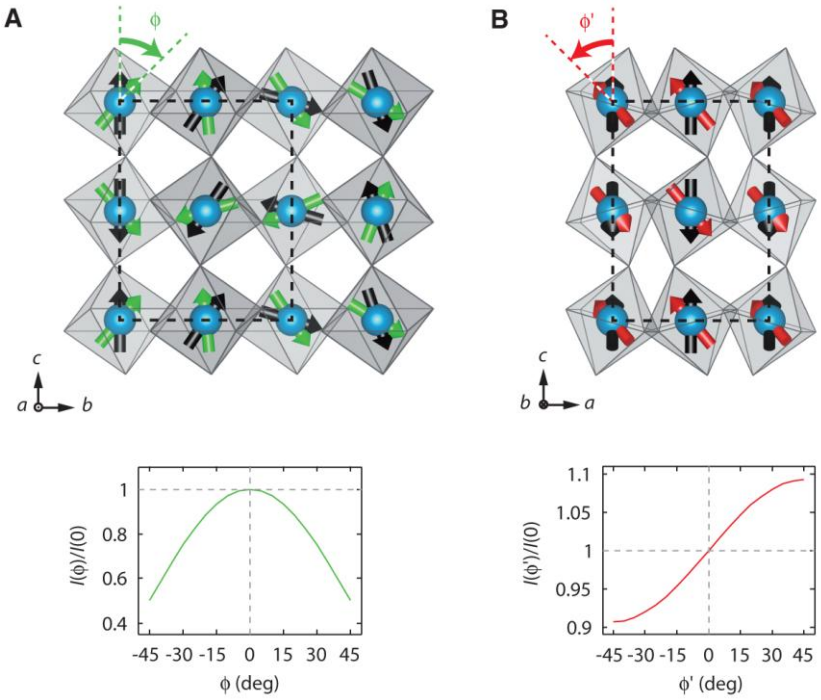

Fig. 3. Spin-motion patterns analyzed to interpret the time-dependent data. The upper panels illustrate the different patterns of how the magnetic structure changes. Black arrows denote how the spins are oriented in the ground state. Color arrows indicate the spin directions at one of the extremes of the excited motion. Tb ions have been removed for clarity. The lower panels show calculations of the changes in (0*q*0) peak intensity as a function of the motion coordinate. (**A**) Antiphase oscillation within the spin cycloid plane, parameterized by using the spin rotation coordinate φ and viewed along the *a* axis. (**B**) Coherent rotation of the spin cycloid plane by an angle φ' about the crystallographic *b* axis viewed along the *b* axis.

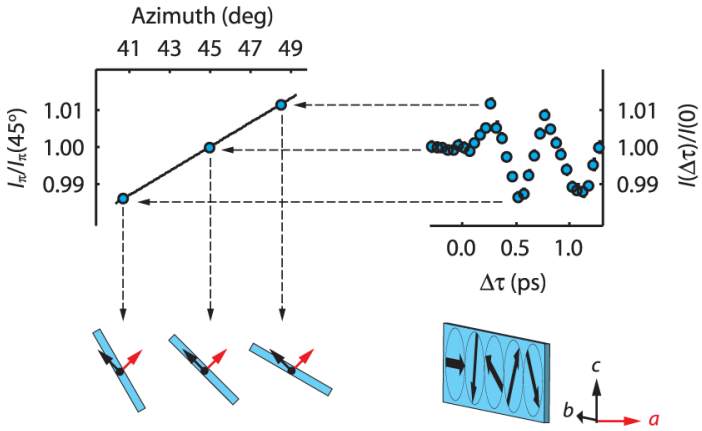

Fig. 4. The diffracted intensity versus spin cycloid rotations. Left: Azimuthal dependence of the (0*q*0) peak for the π-polarized incident x-rays divided by the diffracted intensity at an azimuth of 45°. Right: Time-resolved diffracted intensity normalized to the intensity before excitation. The blue plane represents a plane of a single spin cycloid propagating along the crystallographic *b* axis. The *a* axis is marked with red. The angles of rotation in the drawing have been exaggerated for clarity.